Interference-Free Analysis Using Three-Way Fluorescence Data and the Parallel Factor Model. Determination of Fluoroquinolone Antibiotics in Human Serum

5 authors, including:

Arsenio Muñoz de la Peña
Universidad de Extremadura
208 PUBLICATIONS **5,614** CITATIONS

SEE PROFILE

Anunciación Espinosa-Mansilla
Universidad de Extremadura
134 PUBLICATIONS **3,928** CITATIONS

SEE PROFILE

David Gonzalez-Gomez
Universidad de Extremadura
207 PUBLICATIONS **3,406** CITATIONS

SEE PROFILE

Alejandro C. Olivieri
Rosario National University
373 PUBLICATIONS **11,331** CITATIONS

SEE PROFILE

Some of the authors of this publication are also working on these related projects:

Strategies of multiway calibration for the enhancement of analytical methodologies in the bioanalytical, food and environmental fields View project

Proyecto de Investigación (2017-20): Las emociones en el aprendizaje de Ciencias de la Naturaleza en Educación Primaria. Programa metacognitivo de intervención emocional con alumnado y profesorado en formación View project

Interference-Free Analysis Using Three-Way Fluorescence Data and the Parallel Factor Model. Determination of Fluoroquinolone Antibiotics in Human Serum

**Arsenio Muñoz de la Peña,*,† Anunciación Espinosa Mansilla,† David González Gómez,†
Alejandro C. Olivieri,‡ and Héctor C. Goicoechea§**

*Departamento de Química Analítica, Facultad de Ciencias, Universidad de Extremadura, 06071 Badajoz, España,
Departamento de Química Analítica, Facultad de Ciencias Bioquímicas y Farmacéuticas, Universidad Nacional de Rosario,
Suipacha 531, Rosario, S2002LRK, Argentina, and Cátedra de Química Analítica I, Facultad de Bioquímica y Ciencias
Biológicas, Universidad Nacional del Litoral, Paraje El Pozo, Santa Fe 3000, Argentina*

**Three-way fluorescence data and multivariate calibration
based on parallel factor analysis (PARAFAC) are com-
bined for the simultaneous quantitation of three fluoro-
quinolone anitibiotics (norfloxacin, enoxacin, and oflox-
acin) in human serum samples. The three analytes can
be adequately determined with limits of detection of 0.2,
3.0, and 0.5 μg L^{-1}, respectively, with minimum experi-
mental effort. The selected analytical methodology fully
exploits the so-called second-order advantage of the
employed three-way data, allowing obtaining individual
concentrations of calibrated analytes in the presence of
any number of uncalibrated (serum) components. In
contrast to PARAFAC, less satisfactory results were
obtained with a multidimensional partial least-squares
(nPLS) model trained with the same calibration set.**

High-order tensors of data are particularly useful for the
quantitative analysis of complex multicomponent samples, and
specifically, third-order tensors are gaining widespread analytical
acceptance.[1] The latter are also called three-way data, and are
characterized by following the trilinear or parallel factor analysis
(PARAFAC) model.[2] Interestingly, the decomposition of a three-
dimensional cube of data is unique, allowing relative concentra-
tions and spectral profiles of individual sample components to be
extracted directly. Unlike other high-order calibration methods,
such as *n*-way partial least-squares (*n*PLS),[2] PARAFAC allows for
the quantitation of calibrated constituents in the presence of any
number of uncalibrated species and for the analysis of mixtures
when separation is difficult or time-consuming.

Although three-way techniques are appealing for the analysis
of complex biological samples, applications to real problems have
been relatively scarce. On one hand, three-way data are currently
available to the analyst, thanks to the implementation of hyphen-
ated analytical techniques, but unfortunately, most of them do not
follow the trilinear model. On the other hand, algorithms for
proper data analysis are freely available, yet they are not of simple
use for the average analytical chemist.

Excitation−emission fluorescence matrices (EEMs) produce
three-way data which present certain advantages: measurements
may be conveniently carried out on a single instrument, fluores-
cence signals are sensitive and selective, and the obtained data
are trilinear, and thus, the PARAFAC model is applicable. While
unidimensional fluorescence emission spectra have been widely
employed for the analysis of biologically relevant compounds,[3−7]
application of EEMs in the biomedical field is very sparse.[8,9]
Previous works employing EEMs for quantitative analysis have
been devoted mainly to polycyclic aromatic hydrocarbons.[10−13]
Recently, the quantitation of thiphenyltin in seawater[14] and of six
chlorophyls and pheopigments have been discussed using three-
way fluorescence data on artificial samples.[15]

In this report, we turn our attention to the EEM-based analysis
of fluoroquinolone antibiotics in human serum. Quinolones are
an important group of synthetic antibiotics with antibacterial
action, but the introduction of the fluorinated quinolones repre-
sents important therapeutic advantages, because this group of
antibiotics shows higher antibacterial activity.[16] They are widely

† Universidad de Extremadura.
‡ Universidad Nacional de Rosario.
§ Universidad Nacional del Litoral.
(1) Booksh, K. S.; Kowalski, B. R. *Anal. Chem.* **1994,** *66,* 782A−791A.
(2) Bro, R. *Chemom. Intell. Lab. Syst.* **1997,** *38,* 149−171.

(3) Goicoechea, H. C.; Olivieri, A. C. *Anal. Chem.* **1999,** *71,* 4361−4368.
(4) Damiani, P. C.; Borraccetti, M. D.; Olivieri, A. C. *Anal. Chim. Acta* **2002,**
471, 87−96.
(5) Durán Merás, I.; Muñoz de la Pena, A.; Rodríguez Cáceres, M. I.; Salinas
López, F. *Talanta* **1998,** *45,* 899−907.
(6) Muñoz de la Peña, A.; Moreno, M. D.; Durán Merás, I.; Salinas, F. *Talanta*
1996, *43,* 1349−1356.
(7) Durán Merás, I.; Espinosa Mansilla, A.; Rodríguez Gómez, M. J.; Salinas
López, F. *Talanta* **2001,** *55,* 623−630.
(8) Arancibia, J. A.; Olivieri, A. C.; Escandar, G. M. *Anal. Bioanal. Chem.* **2002,**
374, 451−459.
(9) Hergert, L. A.; Escandar, G. M. *Talanta,* in press.
(10) Muroski, A. R.; Booksh, K. S.; Myrick, M. L. *Anal. Chem.* **1996,** *68,* 3534−
3538.
(11) Booksh, K. S.; Muroski, A. R.; Myrick, M. L. *Anal. Chem.* **1996,** *68,* 3539−
3544.
(12) Beltrán, J. L.; Ferrer, R.; Guiteras, J. *Anal. Chim. Acta* **1998,** *373,* 311−
319.
(13) Wentzell, P. D.; Nair, S. S.; Guy, R. D. *Anal. Chem.* **2001,** *73,* 1408−1415.
(14) Saurina, J.; Tauler, R. *Analyst* **2000,** *125,* 2038−2043.
(15) Moberg, L.; Robertsson, G.; Karlberg, B. *Talanta* **2001,** *54,* 161−170.
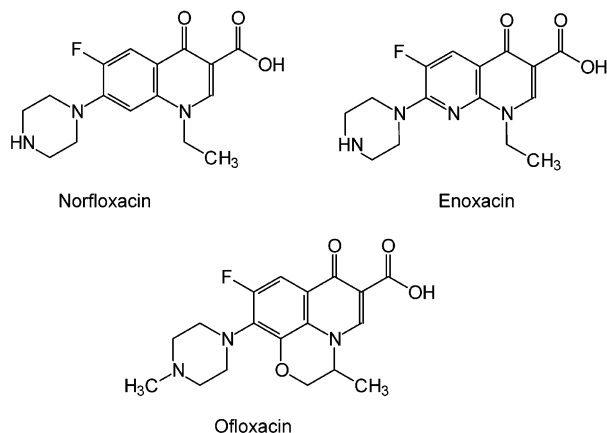
Figure 1. Structures of the studied analytes.

used to treat human and veterinary diseases and also to prevent diseases in food producing animals.[17–19] Their main excretion pathway is urinary, and low amounts are found in plasma; usual therapeutic levels are on the order of 5 mg L^{-1} for the fluoroquinolones herein studied.[20] On the other hand, there is concern about the possibility of exposure to low levels of these compounds, resulting in the development of resistance of human pathogens to antibiotics.[21]

The analysis of fluoroquinolones has traditionally been performed using microbiological methods.[22,23] However, these techniques are slow and suffer from poor precision and specificity. High performance liquid chromatography (HPLC) has become an important tool for routine determination of antimicrobial agents in body fluids, with specific emphasis on fluoroquinolones,[24,25] but in the past decade, multivariate techniques have been incorporated to the analytical protocols.[26] In particular, full-spectrum multivariate calibration methods offer the advantage of their speed, because the separation steps may be avoided.

The quinolones of interest are the so-called second-generation or fluoroquinolones, specifically, norfloxacin (NOR), enoxacin (ENO), and ofloxacin (OFL) (Figure 1).

Although several multivariate algorithms have been applied to the analysis of drugs using different analytical signals, only a single paper has been reported on the simultaneous determination of the presently studied fluoroquinolones.[27] In this latter study,

(16) Jackson, L. C.; Machado, L. A.; Hamilton, M. L. *Acta Medica* **1998**, *8*, 58–61.
(17) Currie, D.; Lynas, L.; Kennedy, D. G.; McCaughey, W. J. *Food Addit. Contam.* **1997**, *15*, 651–655.
(18) Ihrke, P. J.; Papich, M. G.; Demanuelle, T. C. *Vet. Dermatol.* **1999**, *10*, 193–204.
(19) Chen, D. K.; McGeer, A.; de Azavedo, J. C.; Low, D. E. *New Engl. J. Med.* **1999**, *341*, 233–239.
(20) Knapp, J. S.; Fox, K. K.; Trees, D. L.; Whittington, W. L. *Emerg. Infect. Dis.* **1997**, *3*, 33–39.
(21) *Food Chemical News*; CRC Press: Washington, DC, 1996; Vol 37, p 21.
(22) Myllyniemi, A. L.; Nuotio, L.; Lindfors, E.; Rannikko, R.; Niemi, A.; Backman, C. *Analyst* **2001**, *126*, 641–646.
(23) Choi, J.; Yee, A. J.; Thompson, D.; Samoluk, J.; Mitchell, M.; Black, W. D. *J. AOAC Int.* **1999**, *82*, 1407–1412.
(24) Wallis, S. C.; Charles, B. G.; Gahan, L. R. *J. Chromatogr., B: Biomed. Sci. Appl.* **1995**, *674*, 306–309.
(25) Carlucci, G. *J. Chromatogr., A* **1998**, *812*, 343–367.
(26) Levine, B. K. *Anal. Chem.* **1998**, *70*, 209R–228R.
(27) Espinosa-Mansilla, A.; Muñoz de la Peña, A.; Salinas, F.; González Gómez, D. Communication presented at the 10th Jornadas de Análisis Instrumental, Barcelona, 2002, Communication no. PO-BIO-25, Abstract book, page 327.

they were simultaneously determined in human urine samples by combining unidimensional analytical signals (fluorescence emission spectra) and partial least-squares (PLS) calibration. In human serum, however, the proposed determination procedure was unsatisfactory as a result of the high fluorescence intensity of normal serum components in the useful spectral ranges and the presence of low analyte concentrations.

The purpose of the present report is 2-fold. On one hand, EEM data and PARAFAC show up as an extremely useful combination for the simultaneous quantitative determination of fluoroquinolone antibiotics in human serum, with minimum effort from the experimental point of view. On the other hand, the results contribute to the widespread acceptance and use of trilinear fluorescence data, which hold immense potential applications in biomedically oriented analysis. In particular, they avoid the construction of large training sets of samples for the convenient monitoring of therapeutic drugs in biological fluids. In comparison, methods such as PLS would require considerably larger experimental efforts.[3,28,29]

EXPERIMENTAL SECTION

Apparatus. All fluorescence measurements were carried out on an Aminco Bowman series 2 spectrofluorophotometer, equipped with a 150-W Xe lamp, connected to a PC Pentium III microcomputer running under Windows 98 (through a GPIB IEEE-488 interface). Data acquisition and analysis were performed by the use of AB2 software. In all cases, 1.00-cm quartz cells were used.

Reagents. All solvents used were of analytical quality. Norfloxacin, enoxacin, and ofloxacin were purchased from Sigma-Aldrich (Spain). Stock solutions of each compound (100 μg mL^{-1}) were prepared by dissolving them in ethanol (avoiding exposure to direct light and maintaining the solutions at 4 °C). A 0.1 mol L^{-1} sodium acetate/acetic acid buffer solution (pH = 4.0) was prepared from analytical reagents purchased from Panreac (Spain). A stock solution of sodium dodecyl sulfate (SDS) containing 0.1 mol L^{-1} was prepared by dissolving the compound in ultrapure water.

Analytical Methodology. The analysis of mixtures of NOR, ENO, and OFL by conventional spectrofluorimetry is not feasible, because the emission spectra of the three compounds consist of broad spectral bands that significantly superimpose over each other. The selectivity can be increased in a micellar medium composed of sodium dodecyl sulfate (SDS), in which a notable increment in the fluorescence yield is also obtained. A concentration of 1.2×10^{-2} mol L^{-1} of SDS was reported as the optimum for the simultaneous determination of the three fluoroquinolones.[27] Further, since the three analytes are weak acids and their fluorescence spectra depend on the degree of protonation, the overlap among emission spectra was analyzed at two pH values (4.0 and 7.3), which ensures that they exist in their protonated and deprotonated forms, respectively. The study was performed by collecting a total luminescence spectrum for each of the compounds in the form of emission–excitation matrices, concluding that at pH = 4.0, the degree of overlapping is minimal, and hence, this pH is recommended for performing the simultaneous determination.

(28) Goicoechea, H. C.; Muñoz de la Peña, A.; Olivieri, A. C. *Anal. Chim. Acta* **1999**, *384*, 95–103.
(29) Zhang, L.; Small, G. W.; Arnold, M. A. *Anal. Chem.* **2002**, *74*, 4097–4108.

In the above-mentioned chemical conditions, maximum information on the three fluoroquinolones can be scanned in the region $\lambda_{em} = 360-540$ nm ($\lambda_{exc} = 277$ nm), and excitation and emission slits maintained at 4 and 8 nm, respectively. Spectra were collected every 1 nm. For reasons explained below, excitation−emission matrices were measured every 3 nm in the emission range 378−501 nm and every 5 nm in the excitation range 260−330 nm, making a total of $42 \times 15 = 630$ data points.

Calibration and Test Sets. A 15-sample set was built for calibration with the PLS-1, nPLS, and PARAFAC models. The analyte concentrations corresponded to a central composite design (see Supporting Information, Table 1), formed by a three-component full-factorial design at two levels (i.e., $2^3 = 8$ samples), a central point (one sample), and a star design ($2 \times 3 = 6$ samples), making a total of 15 samples (samples C1 to C15). The extreme concentrations for the design were as follows: norfloxacin, $0.00-25.00$ μg L^{-1}, enoxacin, $0.00-300.00$ μg L^{-1}, and ofloxacin, $0.00-80.00$ μg L^{-1}. They were obtained starting from the stock solutions (see above); diluting with water to get intermediate solutions (1.00 μg mL^{-1}); and finally, preparing the samples by dilution with water. Therefore, the content of ethanol in the final samples was $<0.05\%$. All samples contained a concentration of 1.2×10^{-2} mol L^{-1} of SDS and an acetic acid/acetate buffer (pH = 4.0).

Additionally, eight ternary samples (T1-T8) were built with analyte concentrations different from those employed for calibration but within their corresponding calibration ranges (see Supporting Information, Table 1). Emission spectra and EEMs were measured in random order. Data for the synthetic samples T1−T8 were measured on days different from those corresponding to calibration.

Serum Samples. Eighteen serum samples were spiked with the three analytes and diluted with water (1:150), so that the final analyte concentrations were within the calibration ranges (specific details are given below). The samples belonged to different individuals and were collected on different days from healthy volunteer individuals at a local health institution. Their EEMs were registered in random order, and on days different from the calibration/test samples. All samples contained a final concentration 1.2×10^{-2} mol L^{-1} of SDS and an acetic acid/acetate buffer (pH = 4.0). The level of serum dilution implies that the analyte concentrations are being probed in the ranges $0-4$ mg L^{-1} for NOR, $0-45$ mg L^{-1} for ENO, and $0-12$ mg L^{-1} for OFL.

Theory. Three-way Trilinear Data. When a sample produces a $J \times K$ data matrix (a second-order tensor), such as an EEM (J = number of emission wavelengths, K = number of excitation wavelengths), the corresponding set obtained by "stacking" the training matrices is a cube (see Supporting Information, Figure 1). Appropriate dimensions of such a cube are $I \times J \times K$ (I = number of samples). Since EEMs follow a trilinear model, the cube can be written as a sum of tensor product of three vectors for each fluorescent component. If $\mathbf{A}_n$, $\mathbf{B}_n$, and $\mathbf{C}_n$ collect the relative concentration ($I \times 1$), emission ($J \times 1$), and excitation ($K \times 1$) profiles for component n, respectively, the data cube $\mathbf{F}$ can be written as[30,31]

$$\mathbf{F} = \sum_{n=1}^{N} \mathbf{A}_n \otimes \mathbf{B}_n \otimes \mathbf{C}_n + \mathbf{E} \tag{1}$$

where $\otimes$ indicates the tensor product, N is the total number of fluorescent components, and $\mathbf{E}$ is a residual error term of the same dimensions as $\mathbf{F}$. The column vectors $\mathbf{A}_n$, $\mathbf{B}_n$, and $\mathbf{C}_n$ are usually collected into the three loading matrices $\mathbf{A}$, $\mathbf{B}$, and $\mathbf{C}$.

A characteristic property of $\mathbf{F}$ is that it can be uniquely decomposed, providing access to spectral profiles ($\mathbf{B}$ and $\mathbf{C}$) and relative concentrations ($\mathbf{A}$) of individual components in the I mixtures, whether they are chemically known or not. This constitutes the basis of the so-called second-order advantage ("second-order" refers to the tensor order of a single sample data matrix, in contrast to "third-order", as referred to the cube formed by the matrices of I samples). Theoretically, this property should allow the analyst to obtain the concentration values of calibrated constituents in the presence of any number of uncalibrated components.

Several methods exist for the convenient analysis of third-order data, notably PARAFAC,[2] self-weighted alternating trilinear decomposition (SWATLD),[32] and generalized rank annihilation (GRAM).[33] The first two are guided by a least-squares minimization of a certain objective function, whereas GRAM operates by directly solving an eigenvalue/eigenvector problem. Software for using PARAFAC is easily available on the Internet[34] and is becoming more and more employed by chemometricians and analytical spectroscopists.

In what follows, we will mainly employ the PARAFAC model for analyzing the experimental three-way data, although samples of simple composition will be studied by means of nPLS. In the latter method, the three-way array of independent variables is decomposed into a trilinear model, which, however, is not fitted in a least-squares sense. According to the philosophy of PLS, it intends to describe the covariance of the dependent and the independent variables. Although the nPLS model is unique, the uniqueness in this case does not imply that real underlying phenomena, such as pure analyte spectra can be recovered, because the model assumptions do not reflect any fundamental or theoretical model.[35]

Multivariate Calibration with Three-Way Data. Issues relevant to the application of the PARAFAC model to three-way fluorescent data are (1) how to establish the number of fluorophores, (2) how to identify specific fluorescent components from the information provided by the model, and (3) how to calibrate the model in order to obtain absolute concentrations for a particular component in an unknown sample.

The number of responsive components (N) can be estimated by several different methods. The consideration of the PARAFAC internal parameter known as core consistency is a useful technique;[35] however, this procedure is somewhat cumbersome when performed by inexperienced users. In this report, we suggest an intuitive alternative method based on the pseudounivariate calibration line that is obtained by regressing the PARAFAC relative concentration values for the training samples against their standard concentrations. The correct value of N is easily located

(30) Ewing, G. W. *Instrumental methods of chemical analysis*; McGraw-Hill: New York, 1985.
(31) Leurgans, S.; Ross, R. T. *Stat. Sci.* **1992**, *7*, 289−319.
(32) Chen, Z.-P.; Wu, H.-L.; Jiang, J.-H.; Li, Y.; Yu, R.-Q. *Chemom. Intell. Lab. Syst.* **2000**, *52*, 75−86.
(33) Sánchez, E.; Kowalski, B. R. *Anal. Chem.* **1986**, *58*, 496−499.
(34) http://www.models.kvl.dk/source/
(35) Bro, R. Ph.D. Thesis, University of Amsterdam, Netherlands, 1998.

when the linear fit regression error stabilizes as a function of a number of trial components (see below). When the correct number of constituents is reached, the PARAFAC relative concentrations for a given component are linearly related to its nominal concentrations. Introducing more components should lead to a similar (or possibly worse) fit.

Identification of the chemical constituent under investigation is done with the aid of the spectral profiles **B** and **C**, as extracted by PARAFAC, and comparing them with those for a standard solution of the analyte of interest.

Absolute analyte concentrations are obtained after proper calibration, since only relative values (**A**) are provided by decomposing the cube of data. Experimentally, this is done by preparing a set of standards of known composition, which should span the expected variability in actual samples. In the present work, we have chosen to employ a 15-sample design, which appropriately accounts for the presence of the three analytes at hand (see the Experimental Section). Two alternative modes exist for calibration. One of them involves decomposition of the cube formed by the I training mixtures and subsequent use of **B** and **C** for prediction in an unknown sample (see Supporting Information, Table 2). However, this mode does not fully exploit the second-order advantage, because the unknown sample may contain constituents that are not modeled by the calibration set. A second, more useful alternative involves decomposing a cube formed by joining the EEMs for the I training samples with that for the unknown. This latter method was employed in the present report, since it takes advantage of the unique decomposition of the data cube, thus allowing obtaining the concentration of the analyte of interest in the presence of any number of uncalibrated interferents. It should be noticed that employment of this latter mode implies that the cube decomposition should be repeated for each newly analyzed sample.

Figures of Merit. Figures of merit are regularly employed for method comparison. The sensitivity (SEN) for a particular analyte, for example, is estimated as the net analyte signal at unit concentration, whereas the selectivity (SEL) is computed as the ratio between the sensitivity and the total signal, as suggested by Kalivas.[36] More important appears to be the analytical sensitivity, defined, in analogy with univariate calibration, as the ratio between sensitivity and spectral noise

$$\gamma = \mathrm{SEN}/[V(\mathbf{R})]^{1/2} \qquad (2)$$

The inverse (γ^{-1}) establishes the minimum concentration difference that can be appreciated by the method, regardless of the specific technique, equipment, and scale employed.[37] The factor $V(\mathbf{R})$ in eq 2 is the variance of the instrumental signal, which may be estimated by replicate blank measurements.

Standard errors in predicted concentrations $[s(c)]$ have been calculated according to the pseudo-univariate representation provided by PARAFAC.[38,39]

(36) Messick, N. J.; Kalivas, J. H.; Lang, P. M. *Anal. Chem.* **1996**, *68*, 1572−1579.
(37) Cuadros Rodríguez, L.; García Campaña, A. M.; Jiménez Linares, C.; Román Ceba, M. *Anal. Lett.* **1993**, *26*, 1243−1258.
(38) Boqué, R.; Ferré, J.; Faber, N. M.; Rius, F. X. *Anal. Chim. Acta* **2002**, *451*, 313−321.
(39) Faber, N. M.; Bro, R. *Chemom. Intell. Lab. Syst.* **2002**, *61*, 133−149.

$$s(c) = [\mathrm{SEN}^{-2}(1 + h)\,V(\mathbf{R}) + h V(\mathbf{c})]^{1/2} \qquad (3)$$

In eq 3, $V(\mathbf{c})$ is the variance in the measurement of calibration concentrations, usually available to experienced users. Finally, the parameter h is the sample leverage, which gives the position of the sample spectrum in the calibration space and is the same as for a classical zero-order model, that is,

$$h = (c_{\mathrm{unk}} - \bar{c}_{\mathrm{cal}})^2 / \sum_{i=1}^{I} (c_{\mathrm{cal},i} - \bar{c}_{\mathrm{cal}})^2 \qquad (4)$$

where c_{unk} is the predicted concentration for the unknown sample, $c_{\mathrm{cal},i}$ is the ith calibration concentration, and $\bar{c}_{\mathrm{cal}}$ is the mean calibration concentration. The calculation of $s(c)$ provides access to the limit of detection of the method, which can be estimated as[38]

$$\mathrm{LOD} = 3.3 s(0) \qquad (5)$$

where $s(0)$ is the standard deviation in the predicted concentration of the analyte of interest in a blank sample, estimated by setting $c_{\mathrm{unk}} = 0$ in eqs 3 and 4.

Software. All calculations were done using MATLAB 5.3.[40] A routine for PLS-1 was written in our laboratory following a previously known algorithm.[41] Those for nPLS and PARAFAC are available on the Internet,[34] although a useful MATLAB graphical interface was developed in the present work for easy data manipulation and graphics presentation. This interface provides a simple means of loading the data matrices into the MATLAB working space before running PARAFAC. The **B** and **C** profiles provided by the latter are separately plotted in order to allow users to identify the analyte of interest. The pseudo-univariate calibration graph corresponding to this particular component is then displayed, along with the regression error, which is subsequently employed for estimating the correct number of components. Once this is done, the results are conveniently shown in terms of predicted concentration and analytical figures of merit. The MATLAB interface code is available from the authors on request.

RESULTS AND DISCUSSION
Excitation−Emission Fluorescence Matrices. Figure 2A shows the three-dimensional plot corresponding to the EEM for the training sample C1 in wide spectral emission and excitation ranges, showing the presence of both Rayleigh and Raman scatterings, as well as the second harmonic from the diffraction grating. Better insight is gained by considering the corresponding contour plot shown in Figure 2B. To avoid the presence of signals that are uncorrelated with the target concentrations of the studied analytes, EEMs were in all cases recorded in the sensible excitation and emission ranges shown in Figures 2B and 3A, where only the analytes contribute to the overall fluorescence intensity, that is, emission from 378 to 501 nm at 3-nm intervals ($J = 42$ data points) and excitation from 260 to 330 nm at 5-nm intervals ($K = 15$ data points), making a total of 630 spectral points.

(40) MATLAB 5.3, The MathWorks Inc., Natick, MA, 1999.
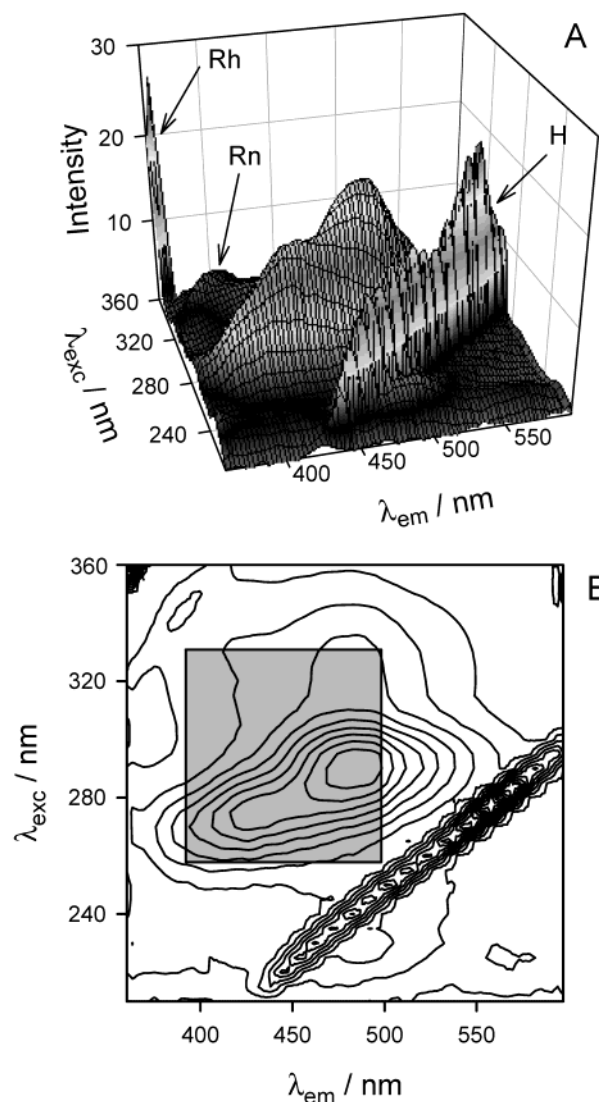(41) Haaland, D. M.; Thomas, E. V. *Anal. Chem.* **1988**, *60*, 1193−1202.

Figure 2. (A) Three-dimensional plot of the EEM for sample C1, showing the presence of a diffraction grating harmonics (H) and Rayleigh (Rh) and Raman (Rn) scatterings, as indicated. (B) Contour plot for the same EEM. The gray rectangle illustrates the spectral excitation and emission ranges selected for calibration with PARAFAC.
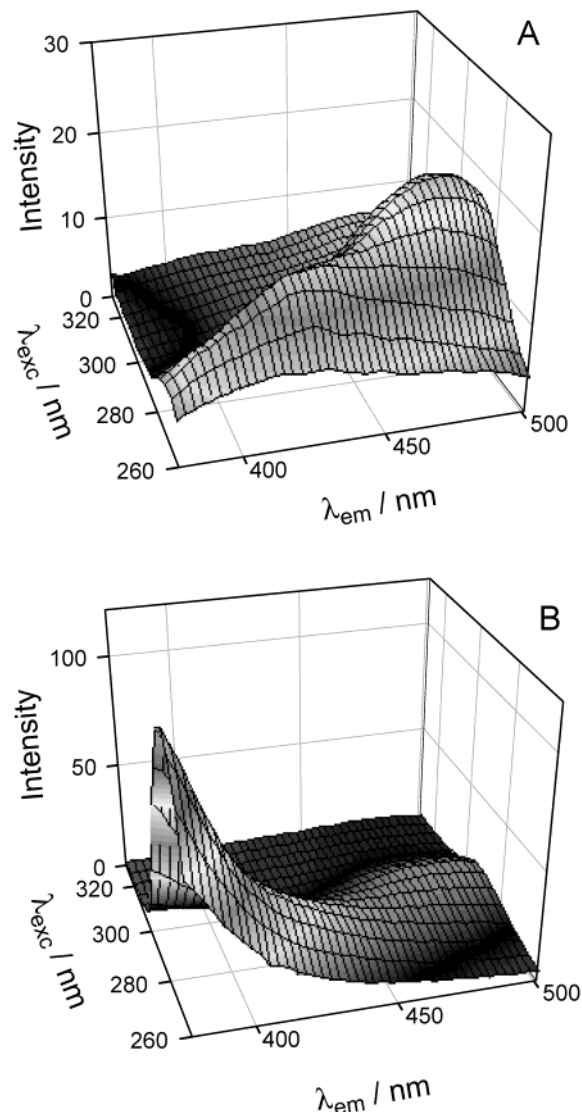

Figure 3. (A) Three-dimensional plot of the EEM for sample C1 recorded in restricted excitation and emission wavelength ranges. (B) Plot of the EEM for the spiked serum sample, S9, for comparison with (A). Notice the difference in vertical scales between (A) and (B).

Figure 3B shows the EEM for one of the spiked serum samples (S9), recorded in the restricted spectral regions mentioned above. Comparison of the vertical scales of Figure 3A and B highlights the significantly larger fluorescence intensity of the serum components in comparison with that for a training sample. As can be seen, the overlapping is very strong in the useful spectral regions, posing significant challenges on the employed analytical technique.

Test Set Results. Unidimensional fluorescence emission data recorded for the calibration samples (at the compromise excitation wavelength of 277 nm) were first analyzed using the PLS-1 method. Appropriate wavelength ranges for each analyte were first selected by computing the calibration variance within a moving-window strategy.[42] These ranges are given in Table 1 and are close to the emission maximums for each of the analyzed components. Leave-one-out cross-validation was then applied to the set of

calibration samples, leading to an optimum numbers of factors equal to four in all cases, as estimated according to Haaland's criterion.[41] Prediction on the eight test samples T1–T8 using this PLS-1 model led to reasonably good recoveries, as shown in Table 1, with slightly worse results for ENO, which is the less responsive analyte.

Three-way EEM data for the test set of samples T1–T8 were also analyzed by nPLS and PARAFAC, in the latter case using the calibration mode that exploits the second-order advantage. Specific details as to the implementation of this mode will be given below in connection with the study of serum samples, where all its potentiality based on the second-order advantage will be adequately displayed. Indeed, for the set of artificial samples composed of only NOR, ENO, and OFL, PARAFAC calibration modes 1 and 2 give comparably good results. Table 1 summarizes the prediction ability of nPLS and PARAFAC, which can be compared to that shown by PLS-1. In going to three-way data, the recoveries are clearly improved in the case of ENO, but are similar to PLS-1 as regards the other two analytes.

(42) Collado, M. S.; Mantovani, V. E.; Goicoechea, H. C.; Olivieri, A. C. *Talanta* **2000**, *52*, 909–920.

Table 1. Predictions on Artificial Samples Applying Different Calibration Methods

	Method					
	PLS-1[a]		nPLS[b]		PARAFAC[b]	
component	REP, %[c]	av recovery[d]	REP, %[c]	av recovery[c]	REP, %[c]	av recovery[d]
Norfloxacin	6.98	98.3 (11)	6.09	98.0 (6)	6.81	102.6 (7)
Enoxacin	8.10	96.7 (9)	4.05	99.1 (4)	4.64	98.8 (5)
Ofloxacin	5.57	97.1 (4)	5.05	98.6 (4)	6.41	97.3 (3)

[a] Using emission spectra, and selecting the following spectral regions: norfloxacin, 390−440 nm; enoxacin, 360−430 nm; and ofloxacin, 460−540 nm. Four latent PLS-1 variables were used for prediction. [b] Using EEMs recorded in the following spectral ranges: emission, from 381 to 480 nm; interval, 3 nm; and excitation, from 250 to 340 nm; interval, 5 nm. [c] REP = Relative error of prediction. [d] Values between parentheses correspond to the standard deviations computed for the recoveries of the eight test samples.

Serum Sample Results. The results obtained for spiked serum samples clearly illustrates the meaning and usefulness of the second-order advantage. On the basis of models trained with the calibration samples C1−C15, neither PLS-1 nor nPLS (modeled with unidimensional emission spectra and EEMs, respectively) was able to produce acceptable results on samples S1−S18. Specifically, relative errors of prediction (REP) were unacceptably large in all cases. This is undoubtedly due to the presence of fluorescent serum components whose influence has not been taken into account in the calibration set. These components not only exhibit emission intensities that overlap with the fluorescence signals from the analytes (Figure 3A and B), but are also intrinsically variable and, thus, difficult to model if the second-order advantage is not employed.

Although nPLS is an efficient way of handling three-way data such as those presently employed, this regression model cannot be trained by including the unknown sample into the calibration data cube, since concentration information is unavailable for unknowns. For reasons explained above, nPLS does not allow obtaining information on uncalibrated interfering agents, such as serum.

To exploit the second-order advantage of three-way data, PARAFAC was separately applied to cubes of data formed by the EEMs for the 15 calibration samples C1−C15, together with each of the serum samples S1−S18 shown in Table 2. Hence, the size of each of the cubes submitted to PARAFAC analysis was 16 × 42 × 15 in all cases (i.e., $I \times J \times K$).

The selection of the number of spectral components in each of these cubes deserves a discussion. As mentioned above, PARAFAC core consistency analysis is a useful tool for this purpose. Figure 4 plots the values obtained for the 16-sample cube when studying sample S9 (Table 2) as a function of a trial number of components. As can be seen, the core consistency drops to a very low value when using five spectral components to model the cube, suggesting that $N = 4$ is a sensible choice.[35] However, as discussed above, an alternative and appealing approach is to consider the regression error of the pseudo-univariate calibration (this procedure should be carried out for each unknown sample). Figure 4 clearly shows that in the case of sample S9, the regression error for the three analytes is stabilized after four spectral components, in agreement with the above analysis. For

Table 2. Results Obtained When Applying PARAFAC Analysis to Serum Samples Spiked with Norfoxacin, Enoxacin, and Ofloxacin

	Norfloxacin μg L^{−1}		Enoxacin μg L^{−1}		Ofloxacin μg L^{−1}	
sample	actual	predicted[a]	actual	predicted[a]	actual	predicted[a]
S1	10.00	6.88 (0.05)	80.00	66.8 (0.9)	20.00	17.1 (0.1)
S2	10.00	7.98 (0.05)	120.00	114.9 (0.9)	35.00	30.1 (0.1)
S3	10.00	10.54 (0.05)	160.00	150.2 (0.9)	50.00	43.7 (0.1)
S4	0.00	0.20 (0.05)	200.00	178.5 (0.9)	65.00	64.1 (0.1)
S5	10.00	8.60 (0.05)	80.00	71.9 (0.9)	0.00	0.2 (0.1)
S6	14.00	11.45 (0.05)	80.00	70.4 (0.9)	0.00	0.3 (0.1)
S7	0.00	−0.34 (0.05)	80.00	69.8 (0.9)	0.00	−0.1 (0.1)
S8	10.00	6.97 (0.05)	120.00	115.7 (0.9)	20.00	16.2 (0.1)
S9	10.00	7.96 (0.05)	50.00	41.6 (0.9)	20.00	19.7 (0.1)
S10	10.00	10.94 (0.05)	350.00	340.9 (1.0)	20.00	21.2 (0.1)
S11	10.00	12.72 (0.05)	0.00	0.7 (1.0)	20.00	22.5 (0.1)
S12	20.00	17.10 (0.06)	0.00	−0.4 (1.0)	20.00	23.6 (0.1)
S13	12.00	11.85 (0.05)	0.00	1.0 (1.0)	20.00	23.0 (0.1)
S14	12.00	9.92 (0.05)	0.00	−0.3 (1.0)	20.00	17.1 (0.1)
S15	5.00	6.50 (0.05)	40.00	42.2 (1.0)	20.00	17.8 (0.1)
S16	20.00	15.67 (0.05)	48.00	35.4 (0.9)	20.00	23.0 (0.1)
S17	20.00	17.40 (0.05)	68.00	48.2 (0.9)	20.00	23.6 (0.1)
S18	5.00	5.00 (0.05)	60.00	61.4 (0.9)	20.00	18.7 (0.1)
		statistical results[b]				
RMSEP		2.17		9.9		2.9
REP%		17.4		6.6		7.3

[a] Standard deviation in parentheses. In all cases, the number of spectral components is four. [b] RMSEP, root-mean-square error of prediction; REP%, relative error of prediction.
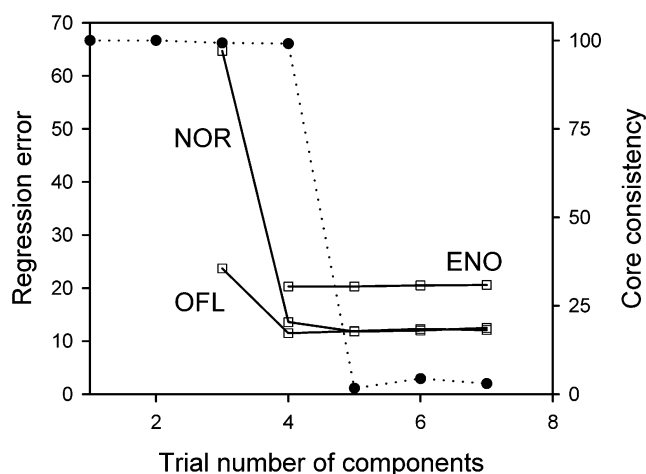

Figure 4. Dotted line, plot of the PARAFAC core consistency values as a function of the trial number of components for the cube composed of the EEM for sample S9 and the 15 calibration EEMs. Solid lines, regression errors for the PARAFAC pseudo-univariate calibration graphs generated for each of the three analytes after processing the same data cube, as indicated. Notice that the less responsive analyte ENO does not appear in the model if the number of components is set to less than four.

the remaining serum samples shown in Table 2, the estimated number of components was also four, showing that although the calibration samples were built starting from the three pure analytes, the presence of serum adds new fluorescent constituents to the data cube, collectively considered as a single extra component by PARAFAC.

As regards the loading matrices provided by PARAFAC when processing sample S9 together with the calibration set, profiles **B** and **C** are plotted in Figure 5A and B, where the components
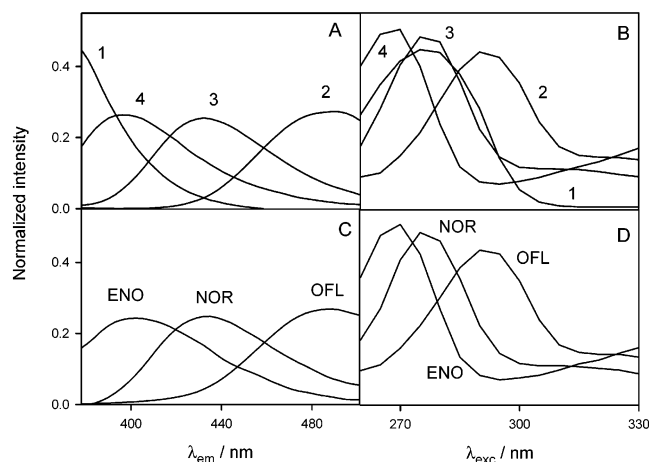
Figure 5. (A) Emission profiles provided by a four-component PARAFAC model (**B** matrix) used to process the cube formed by sample S9 and the 15 calibration samples. The components are labeled according to the contribution of the overall variance. (B) Excitation profiles (**C** matrix). (C) Normalized experimental emission spectra for the three studied analytes, as indicated, using $\lambda_{exc} = 277$ nm. The spectra were recorded every 3 nm in the same spectral range as in (A) for proper comparison. (D) Normalized experimental excitation spectra (at $\lambda_{em} = 435$, 400, and 485 nm for NOR, ENO, and OFL, respectively), recorded every 5 nm in the same spectral range as in (B). All experimental solutions are at pH = 4.0 and contain SDS at 1.2×10^{-2} mol L^{-1}.

have been labeled according to the order assigned by the model in the specific cube under investigation. They appear in the order of their contribution to the overall variance, and in this particular case, the interference appears in the first place, indicating that it is the main source of fluorescence intensity across this particular data cube. Comparison with the experimental emission and excitation spectra shown in Figure 5C and D for solutions of pure standards allows one to ascribe component no. 1 to serum, no. 2 to OFL, no. 3 to NOR, and no. 4 to ENO.

The prediction results for the serum samples are listed in Table 2. A positive bias is found in the determination of ENO, which is understandable, since the latter is the least responsive of the three studied components. However, the statistical analysis shows mean prediction errors for all three analytes that are comparable to those found in the artificial samples T1−T8. This is a remarkable achievement, since successful prediction for specific analytes in samples of the complexity of human serum usually requires large calibration sets when unidimensional spectra are employed. For the sake of comparison, the following three PLS-1-based determinations can be cited, requiring 80 different serum samples for theophylline from UV−vis spectrophotometry,[28] 50 sera for tetracycline using fluorescence emission,[3] and more than 100 for glucose by near-infrared spectroscopy.[29]

Figures of Merit. The study based on PARAFAC pseudo-univariate calibration also furnishes interesting figures of merit. The standard errors in predicted concentrations have been reported in Table 2, using, as ancillary information, $V(R) = 0.25$ squared fluorescence units, $V(c)$ estimated from error propagation in prepared concentrations as $\sim 1 \times 10^{-4}$ μg^2 L^{-2}, analyte sensitivities (see below), and sample leverages. Values range from 0.05 to 0.1 $\mu g\ L^{-1}$.

Table 3. Analytical Figures of Merit

figure of merit[a]	Norfloxacin	Enoxacin	Ofloxacin
sensitivity (SEN), FU L μg^{-1}	9.7	0.6	4.4
selectivity (SEL)	0.70	0.58	0.87
analytical sensitivity (γ), L μg^{-1}	20	1.1	10
γ^{-1}, $\mu g\ L^{-1}$	0.05	0.9	0.1
LOD, $\mu g\ L^{-1}$	0.2	3.0	0.5

[a] FU, fluorescence units (arbitrary).

Other analytical figures of merit are collected in Table 3. As can be seen, the more demanding analyte is ENO, which shows lower sensitivity and selectivity, with a consequently larger limit of detection and γ^{-1} than either NOR or OFL. Converting the limits of detection shown in Table 3 to serum levels implies values of 30 $\mu g\ L^{-1}$ for NOR, 450 $\mu g\ L^{-1}$ for ENO, and 75 $\mu g\ L^{-1}$ for OFL. These results can be successfully compared to those for usual liquid chromatographic procedures with UV−visible detection, which have a limit of detection in serum in the range of 20−100 $\mu g\ L^{-1}$.[24,25]

Overall, the results should be considered as satisfactory in view of the complexity of the studied samples.

CONCLUSIONS

The results presented in this report indicate that the combination of fluorescence excitation−emission measurements and the parallel factor model of three-way data is a highly useful technique for the analysis of complex samples, on the condition that the so-called second-order advantage is adequately exploited. The simultaneous determination of three fluoroquinolone antibiotics in human serum, although satisfyingly successful, is only a limited example of the immense potentiality of these methods in the biomedical analytical fields. Future prospects will undoubtedly involve samples of similar or higher complexity, with the aim of placing three-way data within the realm of routine analytical spectroscopy.

SUPPORTING INFORMATION AVAILABLE

Schematic representation of three-way data and calibration details. This material is available free of charge via the Internet at http://pubs.acs.org.